Journal of NeuroVirology (2019) 25:496–507
https://doi.org/10.1007/s13365-019-00750-1

Immunometabolic phenotype of BV-2 microglia cells upon murine cytomegalovirus infection

Natalia Kučić[1] · Valentino Rački[1] · Kristina Jurdana[2] · Marina Marcelić[1] · Kristina Grabušić[2]

Received: 21 December 2018 / Revised: 19 March 2019 / Accepted: 3 April 2019 / Published online: 25 April 2019

Abstract

Microglia are resident brain macrophages with key roles in development and brain homeostasis. Cytomegalovirus (CMV) readily infects microglia cells, even as a possible primary target of infection in development. Effects of CMV infection on a cellular level in microglia are still unclear; therefore, the aim of this research was to assess the immunometabolic changes of BV-2 microglia cells following the murine cytomegalovirus (MCMV) infection. In light of that aim, we established an in vitro model of ramified BV-2 microglia (BV-2$^{\varnothing FCS}$, inducible nitric oxide synthase (iNOS^{low}), arginase-1 (Arg-1^{high}), mannose receptor CD206^{high}, and hypoxia-inducible factor 1α (HIF-1α^{low})) to better replicate the in vivo *conditions* by removing FCS from the cultivation media, while the cells cultivated in 10% FCS DMEM displayed an ameboid morphology (BV-2$^{FCS\ high}$, iNOS^{high}, Arg-1^{low}, CD206^{low}, and HIF-1α^{high}). Experiments were performed using both ramified and ameboid microglia, and both of them were permissive to productive viral infection. Our results indicate that MCMV significantly alters the immunometabolic phenotypic properties of BV-2 microglia cells through the manipulation of iNOS and Arg-1 expression patterns, along with an induction of a glycolytic shift in the infected cell cultures.

Keywords Microglia · Murine cytomegalovirus · BV-2 cells

Introduction

The importance of studying the neurobiology of cytomegalovirus (CMV) infection comes from its association with congenital defects as a result of infection in the developing brain due to an immature immune defense (Naing et al. 2016). Hence, the focus of CMV infection in the central nervous system (CNS) is not only on the neurons but on glia cells as the immune cells in the brain (Van den Pol et al. 2002).

Among glia cells astrocytes are the majorly infected cells, while resident microglia are the first immune cells which are attracted by the cytokines released from infected astrocytes (Rock et al. 2004). However, novel research is pointing out that microglia is perhaps the primary target of infection and that the neuroimmune alterations might be critical for the consequences of infection (Cloarec et al. 2016).

Microglia are the resident brain macrophages originating from the yolk sac in early development (Ginhoux et al. 2010). Although the full spectrum of physiological microglial roles is beginning to be discovered, current evidence indicates functions such as promoting programmed cell death and phagocytosis of apoptotic neurons in development and throughout life (Marín-Teva et al. 2004; Witting et al. 2000). Furthermore, microglia was found to be instrumental in developing, maintaining, or removing synapses (Schafer and Stevens 2013; Miyamoto et al. 2016), thus ensuring proper neuronal function. Finally, microglia constantly monitor their surroundings and ensure homeostasis through their interactions with other brain cells, along with a rapid immunometabolic response to endogenous or exogenous stimuli, such as stroke or viral infections (Tsai et al. 2016; Guruswamy and El Ali 2017; Hanisch and Kettenmann 2007; Das Sarma 2014). However, contrary to popular belief, microglia is constantly in its active form and therefore cannot be assessed effectively through the traditional M1/M2 polarization (Ransohoff 2016), but instead, through integration of immune and metabolic

Electronic supplementary material The online version of this article (https://doi.org/10.1007/s13365-019-00750-1) contains supplementary material, which is available to authorized users.

✉ Natalia Kučić
natalia.kucic@medri.uniri.hr

[1] Department of Physiology and Immunology, Faculty of Medicine, University of Rijeka, Braće Branchetta 20, 51000 Rijeka, Croatia

[2] Department of Biotechnology, University of Rijeka, Radmile Matejčić 2, Rijeka, Croatia

assessments since that only completes the integrity of cellular function (Artyomov et al. 2016). It should be mentioned that immunometabolism is becoming crucial in research of various conditions and as overall response in all immune cells (Mathis and Shoelson 2011). Most research in CMV infections is focused on the immune aspects, although there is a growing area in the metabolic consequences of the infection as well (Loftus and Finlay 2016; Fleck-Derderian et al. 2017).

CMV is a member of the viral family known as Herpesviridae linked to many disorders in the CNS where it induces immune response and microglial activation. Among various species, the murine cytomegalovirus (MCMV) stands out as one of the most commonly used alternative for human cytomegalovirus, being the best characterized and is confirmed as a valuable experimental model for studying the immunobiology of the CMV in CNS (Reddehase and Lemmermann 2018; Jonjic 2015). The viral program starts immediately upon infection in the cascade fashion through at least three phases initiating with the expression of immediate early (IE) proteins responsible for transcription of early viral (E) and late (L) phase proteins required for viral DNA replication and the release of the first viral progeny (Lucin and Jonjić 1995).

It has been shown that microglial cells are a direct target of infection during development with a pivotal role in antiviral defense in the CNS (Kettenmann et al. 2011). CMV drives microglial immune response by inducing a pro-inflammatory microglial state which promotes pathogen clearance (Cheeran et al. 2001). Similar pattern can be seen in early fetal development, with microglia being a prominent CMV target of infection, causing early pro-inflammatory response, formation of microglial nodules, and a possible adverse impact on brain development (Cloarec et al. 2016; Teissier et al. 2014). Novel research focused on in utero administration of drugs targeting microglia has promising results in improving neurodevelopmental outcomes and indicates the importance of microglia and CMV interaction in embryonic infections and developmental disorders (Cloarec et al. 2018).

Due to the lack of in vitro research, the underlying changes on the cellular level are still unclear. With the development of various non-animal research models, particularly cell lines, novel opportunities for constructing more practical research models arise. Thus, using cell type-specific models may give an insight into the varied effects the virus causes in different cell types and, in addition, may contribute to the understanding of phenotype of neurological cells during CMV infection (Doke and Dhawale 2015; Stansley et al. 2012; Slavuljica et al. 2015).

Our research model has included BV-2 microglia cell line with the aim to assess the immunometabolic changes within distinct cell phenotype following MCMV infection.

Materials and methods

Cells, virus, and infection conditions

BV-2 microglia cell line (Blasi et al. 1990; Henn et al. 2009), kindly provided by laboratory of Professor Jasna Križ (Montreal, Canada), was grown in Dulbecco's modified Eagle's medium (DMEM) (PAN Biotech, Aidenbach, DE) without fetal bovine serum (FCS) or supplemented with 10% (*v*/*v*) fetal calf serum (FCS), 2 mM L-glutamine, 100 mg streptomycin, and 100 U penicillin (GIBCO, Gran Island, NY, USA). The cells were cultured in Petri dishes at 37 °C with 5% CO_2 and saturated humidity. Cell viability was assessed using the Countess FL Automated Cell Counter (Thermo Fisher Scientific, Waltham, MA, USA), an automated technique which has been validated for assessing cell viability (Cadena-Herrera et al. 2015). The viability was assessed before each experiment as part of standard protocol and cell counting. We proceeded with the experiment if the cell viability was ≥ 95% in both cultivation conditions.

Primary murine embryonic fibroblasts (MEFs) were generated from BALB/c mice and propagated in minimal essential medium (MEM) supplemented with 5% (*v*/*v*) FCS, 2 mM L-glutamine, 100 mg streptomycin, and 100 U penicillin (GIBCO, Gran Island, NY, USA).

The wild-type MCMV of the Smith strain (VR-194; ATCC) was used as a tissue culture-grown virus. Virus without m138 (Δm138-MCMV), MCMV encoded Fc receptor like protein, was used for immunofluorescence experiments to avoid the unspecific staining, and MCK-2 repaired MCMV/MCK-2 revertant virus (tissue culture derived WT MCMV reconstituted from BAC pSM3fr-MCK-2fl) (Jordan et al. 2011) was used to estimate the effectiveness of microglia infection (kindly provided by Dr. Ilija Brizić from the laboratory of Professor Stipan Jonjić, Medical Faculty, University of Rijeka, Croatia). To achieve a cell monolayer, 10^5 cells per well were seeded in tissue culture plates (Greiner Bio-one, Frickenhausen, DE) and when confluency was reached, cells were infected at m.o.i. of 10 using the centrifugal enhancement of infectivity (18,000 rpm for 30 min).

Reagents and antibodies

Real-time metabolism assay was performed using IFN-γ (Genentech, San Francisco, CA, USA) and FCCP/oligomycin as part of the Cell Energy Phenotype Test Kit (Agilent, Santa Clara, CA, USA). For visualization of MCMV proteins expressed through immediate early/early/late phase the following antibodies were used: CROMA 101 (anti-immediate early phase protein 1 (IE1)) and CROMA 103 (anti-early phase protein 1 (E1)) produced in our laboratory, along with M04.10 (anti-early phase protein (m04)) and M25C.01 (anti-mid/late-phase protein (m25)), kindly

provided by Assistant Professor Vanda Juranić Lisnić from the laboratory of Professor Stipan Jonjić, Rijeka, Croatia). Immunometabolic changes were analyzed by iNOS (Thermo Fisher Scientific, Waltham, MA, USA), Arg-1 (Santa Cruz Biotechnology, Dallas, TX, USA), CD206 (Bio-Rad, Hercules, CA, USA), HIF-1α (Abcam, Cambridge, UK), FITC goat α-mouse CD16/32 (BD Biosciences, Franklin Lakes, NY, USA), and PE rat α-mouse CD86 (BD Biosciences, Franklin Lakes, NY, USA) monoclonal antibodies. Tubulin and actin were labeled using β-tubulin (Thermo Fisher Scientific, Waltham, MA, USA) and β-Actin (Sigma-Aldrich, St. Louis, MO, USA), respectively.

Immunofluorescence staining of immunometabolic markers and/or MCMV proteins was performed with Alexa 488 goat α-mouse IgG_1, Alexa 488 and 555 goat α-rat IgG_{2a}, and Alexa 555 goat α-rabbit secondary reagents (all from Thermo Fisher Scientific, Waltham, MA, USA). Blue-fluorescent DNA stain DAPI was used for nuclear staining (Thermo Fisher Scientific, Waltham, MA, USA). For flow cytometry method FITC goat α-mouse (BD Biosciences, Franklin Lakes, NY, USA) and α-mouse PE rat (BD Biosciences, Franklin Lakes, NY, USA) secondary antibodies were used, as well as HRP conjugated goat α-mouse (Jackson ImmunoResearch, West Grove, PA, USA) for the Western blot technique.

Immunofluorescence

Cells grown in monolayers on glass coverslips in 24-well tissue-culture plates were rinsed with phosphate-buffered saline (PBS), fixed with 4% paraformaldehyde (PFA) for 20 min, permeabilized with 0.1% Triton X-100 for 10 min, and blocked with 2% fetal calf serum in PBS for 30 min. Labeling was done using primary and a coupled secondary antibodies for 1 h at room temperature. For analyzing viral and cell antigens, images were acquired using the fluorescent microscope Olympus BX51 (magnification of 400–×1000). Images were further processed in Image J and signals of fluorescent dots were quantified using imaging software Zen Blue (Zeiss, Oberkocken, DE). All immunofluorescence experiments were repeated a minimum of four times, with a minimum of 10 images from all experiments being analyzed with the Zen Blue software for obtaining the mean fluorescent intensity.

Flow cytometry analysis

Cells were cultured in 12-well tissue culture plates and incubated at 37 °C and 5% CO_2. After the specific incubation period cells were trypsinized, the appropriate neutralization solution was added and cell suspension was immediately centrifuged for 5 min at room temperature at 1500 rpm (Thermo Scientific centrifuge). Cells were then resuspended in FACS buffer and ~100 μL of cell suspensions were divided and added into the appropriate number of tubes (Falcon). Subsequently, 100 μL of the primary and corresponding secondary antibody was added to each tube. Each incubation step was followed by washing step with FACS buffer and centrifugation for 2 min at 2000 rpm. Cells were analyzed by FACSCalibur flow cytometry (BD Biosciences, Franklin Lakes, NY, USA) using The CellQuest Pro (BD Biosciences, Franklin Lakes, NY, USA) program. The results were processed using the Flowing Software (Turku, Estonia) application and are shown as histograms showing the intensity of used fluorescence.

Western blot analysis

Cellular extracts were prepared in RIPA lysis buffer supplemented with protease inhibitor and/or phosphatase inhibitor cocktail set (Roche, Basel, CH).

Proteins were separated by sodium dodecyl sulfate polyacrylamide gel electrophoresis (SDS-PAGE) and blotted onto a PVDF Western blotting membrane (GE Healthcare Limited, Amersham, UK). Membranes were washed in Tris/HCl-buffered saline (TBS), blocked with 5% non-fat milk for 1 h at room temperature, and incubated with primary antibodies at 4 °C overnight. After 1-h incubation at room temperature with horseradish peroxidase-coupled secondary antibodies, signals were detected with enhanced chemiluminescence Amersham ECL Prime Western Blotting Detection Reagent (GE Healthcare Limited, Amersham, UK) according to standard methods.

Virus-titer assay (plaque forming unit)

Cell culture supernatants were collected from infected cells 24 h after infection and transferred to primary MEFs as susceptible cell line generated from BALB/c mice. Number of infectious particles in tissue-culture homogenates was determined by titration on monolayers of subconfluent MEF cultures in 48-well plates using standard viral-plaque assay as described (Reddehase et al. 1994). Titration was carried out in three replicates and results were presented as number of infectious virions (plaque per unit (p.f.u.)) and compared by using the Mann–Whitney *U* test.

Real-time metabolism assay

ECAR and OCR measurements were made with an XF-24 Extracellular Flux Analyzer (Agilent Santa Clara, CA, USA), proven in this cell line (Orihuela et al. 2016). A utility plate containing calibrant solution (1 mL/well) together with the plates containing the injector ports and probes were placed in a CO_2-free incubator at 37 °C over-night. The following day cells were plated at 0.2×10^6 cells/well of a 24-well

Seahorse plate (same-day seeding) with one well per row of the culture plate containing only supplemented media without cells, as a negative control. Before the assay, media was removed from cells and replaced with glucose-, pyruvate-, and glutamine-supplemented XF assay buffer (500 mL/well), and the cell culture plate was placed in a CO_2-free incubator for at least 1 h. Inhibitors (oligomycin and carbonyl cyanide-4-(trifluorome-thoxy)phenylhydrazone (FCCP) were added to the appropriate port of the injector plate. This plate together with the utility plate was run on the Seahorse for calibration. Once complete, the utility plate was replaced with the cell culture plate and run on the Seahorse XF-24. All cultivation conditions were done in quadruplicates to obtain the mean ECAR and OCR values provided in the results.

Statistical analysis

Statistical analysis was performed using Statistica v13 program (TIBCO Software, Palo Alto, CA, USA). After confirming normal distribution using the Kolmogorov-Smirnov test, Student's *t* test was used to compare two independent samples. Signals of fluorescent dots were quantified for each cell by Zen Blue imaging software (Zeiss, Oberkochen, DE), with 10 images analyzed over four experiments per each condition.

Results

Establishing a phenotype model of ramified BV-2 microglia cells

One of the main issues in in vitro microglia research is the constant proinflammatory activated cellular state (Timmerman et al. 2018). Therefore, our first goal was to establish a model of quiescent microglia in order to study further alterations towards its activation mode.

The experiments were performed on the immortalized BV-2 microglia cell line, a proven replacement for the primary microglia. These cells spontaneously show a dual phenotype cultivated in the standard conditions. In order to obtain the homeostatic conditions of microglia in vivo, we modified cultivation conditions to achieve the phenotype with similar morphological and functional characteristics as native microglia.

BV-2 microglia cells are conventionally grown in DMEM supplemented with 10% *v*/*v* serum (10% fetal calf serum (FCS)). After standard cultivation in the 10% DMEM, an ameboid cell form was observed. This kind of morphology is also present after culturing BV-2 microglia cells in the primary microglia cultured medium (not shown). Upon analyzing the cultivation media, we found that one of the prime constituents is Fetuin A, which is a known TLR-4 activator (Pal et al. 2012). Thus, we determined that a change in media composition is needed to induce cell branching correspondent to a ramified shape in the native state of microglia cells. For this purpose, the cells were cultured in the medium without FCS to suppress their constitutive activation under standard cultivation conditions.

Subtracting FCS from the growing medium caused a gradual shift in cell morphology through the time course of 96 h in serum free-media cultivation to a more ramified state (BV-$2^{øFCS}$), while the cells that were cultivated for long term in the standard conditions with 10% FCS (BV-$2^{FCShigh}$) retained an ameboid morphology (Fig 1a). Cells viability in both cultivation conditions was ≥ 95%.

After successful cellular differentiation into a characteristic morphological cell phenotype, the next goal was to define the immune-metabolic functional properties. We utilized the protein expression of molecules that are hallmarks of classical M1 activation state (inducible nitric oxide synthase (iNOS)), alternative M2 activation state (arginase-1 (Arg-1) and mannose Receptor (CD206)) and of metabolic activity (hypoxia inducible factor-1 alpha (HIF-1α)).

The results of the immunofluorescence point to a constitutively high expression of iNOS in BV-$2^{FCShigh}$ cells (Fig. 1b), indicating an increased NO production and associating M1-like cell activation properties, unlike the decrease in iNOS expression present in serum-free cells (BV-2 ^{øFCS}) (Fig. 1b). The opposite is true for the expression pattern of the CD206 and Arg-1 molecules as the M2 anti-inflammatory markers confirm the association of ramified cells with the quiescent M2-like features of the resting cell phenotype. Inclusively, BV-$2^{FCShigh}$ phenotype exhibits the high expression of distinct activation markers, iNOS and HIF-1α, with the low expression of Arg-1 and CD206. This expression pattern was specified as an activated profile (**$iNOS^{high}Arg\text{-}1^{low}CD206^{low}HIF\text{-}1\alpha^{high}$**), while the BV-$2^{∅FCS}$ exhibited a low expression of iNOS and HIF-1α with a high expression of Arg-1 and CD206. Therefore, removing the FCS from the media resulted in a distinctive quiescent cell profile (**$iNOS^{low}Arg\text{-}^{high}CD206^{high}HIF\text{-}1\alpha^{low}$**) (Fig. 1b).

To further characterize these cells, we used a real-time metabolic assay to assess the metabolic status that ended up revealing a dramatic difference. The baseline metabolic potential of BV-$2^{øFCS}$ cells was mostly quiescent with minimal metabolic activity (low OCR and ECAR), while the BV-$2^{FCS\ high}$ cells were glycolytically active (low OCR and high ECAR) (Fig. 1c). Both cell phenotypes had an equal metabolic potential to respond to stimuli when exposed to stressors. Therefore, after stressing the cells with FCCP and oligomycin, there is a shift towards a more energetic state in both cell cultures, with a similar increase of metabolic potential. Particularly high metabolic activity was measured in HIF-1α-positive BV-$2^{FCShigh}$ cells (Fig. 1c), wherein it modulates energy metabolism leading to its inherent effect on the glycolytic rate increase.

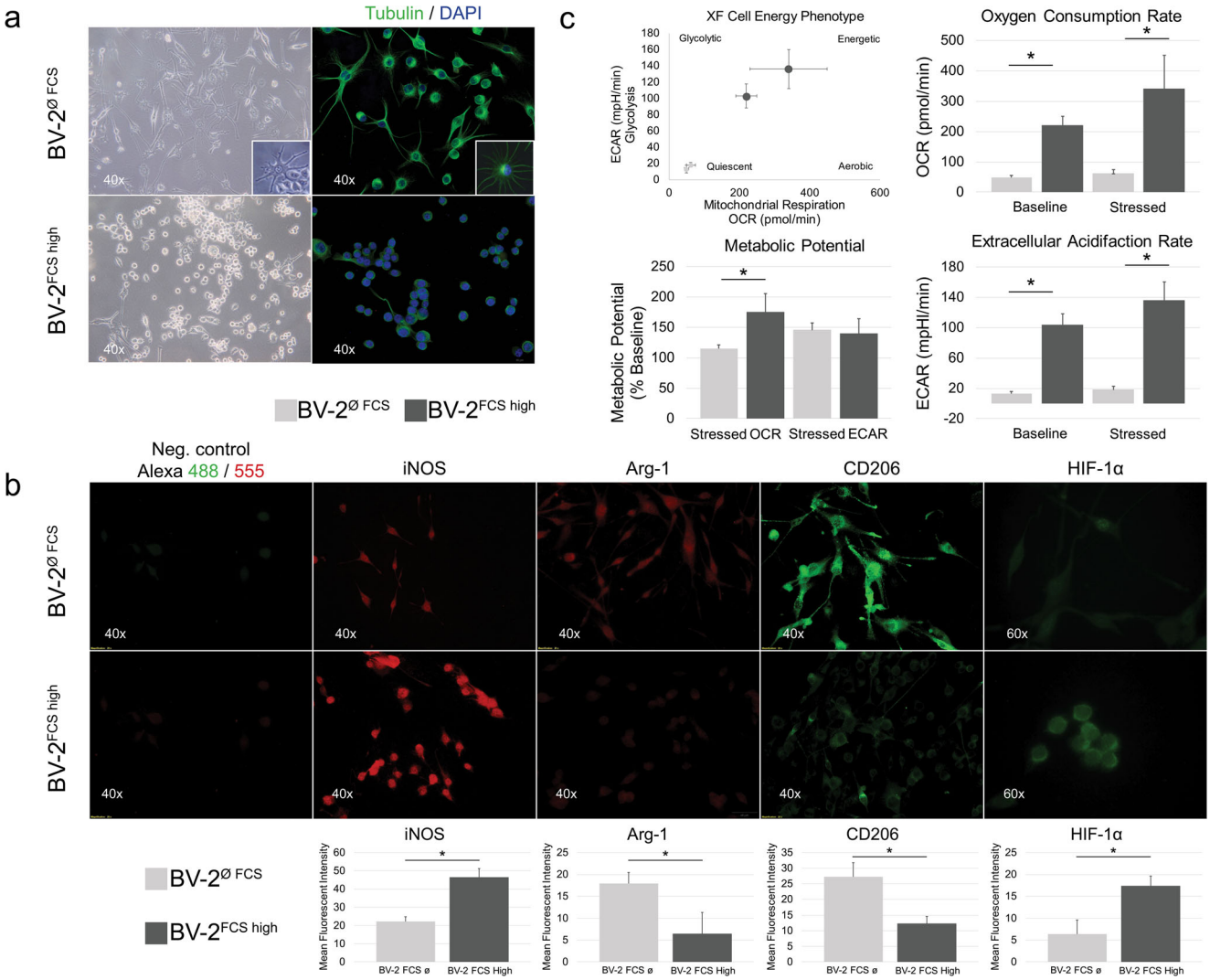

Fig. 1 BV-2 microglia cells uniformed within a distinct phenotype. **a** Different cell morphology phenotype of the murine microglial BV-2 cell line has been shown with the bright field /phase-contrast (*left panel*) and immunofluorescence (IF) (*right panel*) images. The cells were cultivated long term in two different conditions, in the DMEM medium supplemented with 10% FCS (BV-$2^{FCShigh}$) or without FCS (BV-$2^{øFCS}$) for 96 h prior to experiments. Differences in cell shape are clearly visible as BV-$2^{FCS\ high}$ cells retain an ameboid round blob/macrophage-like morphology, while BV-$2^{øFCS}$ shift to ramified/branched/spider-like morphology (visible inside the window box frame). In the IF images tubulin (anti-mouse Ab-conjugated with Alexa 488, green fluorescence) is used for cytoplasmic and DAPI (blue fluorescence) for nucleus staining. **b** Immunofluorescence of BV-2 microglial cells cultivated for 96 h in DMEM without FCS (BV-$2^{Ø\ FCS}$) exhibit distinct quiescent cell phenotype associated with low expression of iNOS and HIF-1α and high expression of Arg-1 and CD206 (iNOS^{low}Arg-1$^{bright/high}$CD206^{high}HIF-1α^{low}), unlike the cells cultivated with 10% FCS supplementation (BV-$2^{FCShigh}$) that exhibit activated phenotype associated with high expression of iNOS and HIF-1α with low expression of Arg-1 and CD206 (iNOS^{high}Arg-1^{low}CD206^{low} HIF-1α^{high}) is specified with distinct markers of activation. IF images (*upper panel*) and quantification analysis below each image (*lower panel*) show in BV-$2^{øFCS}$ in BV-$2^{FCShigh}$. Staining with secondary Abs conjugated with Alexa 488 (green fluorescence) and Alexa 555 (red fluorescence) were used as a negative control. Images magnification was 40–×60. **c** Cell energy phenotype based on real-time metabolism assay of BV-2 microglial cells reveals that the baseline metabolic potential of BV-$2^{ØFCS}$cells (*filled square*) is mostly quiescent (low OCR and ECAR), while the BV-$2^{FCS\ high}$ (*dashed*) cells are glycolytic (low OCR and high ECAR). Cells were cultivated for 96 h in distinct cultivated conditions and after stressing the cells with FCCP and oligomycin there is a shift towards a more energetic state in both cell cultures with a similar increase of glycolytic metabolic potential, while the BV-$2^{FCS\ high}$ exhibit greater aerobic metabolic reserve (*graphical columns*)

BV-2 cell susceptibility to MCMV infection

After cells were uniformed within distinct phenotypes associated with BV-$2^{ØFCS}$ and BV-$2^{FCS\ high}$ we determined the following for both cell types: (i) susceptibility to MCMV infection, (ii) supporting of the viral replication, and (iii) the productivity of infection. We infected the cells prior to the experiments with both MCMV wild-type (wt) Smith strain virus and MCMV/MCK-2 mutant virus to compare the effectiveness of cell infection, since

it has been published that this viral chemokine promotes the infection of the macrophage lineage in vitro and in vivo (Wagner et al. 2013). The percentage of infected cells with both viruses was comparable, so we continued experiments with MCMV wt as a BV-2 cell-sensitive virus. We followed the kinetics of MCMV marker protein expressions to assess the viral capability to infect the cells and complete its replication cycle. The used viral protein markers covered the three phases of the virus replication cycle, starting from the immediate-early protein (IE1/gp89), which was expressed in the cell nucleus (Busche et al. 2008) and detected as two abundant Western blot bands previously well characterized as phosphorylated IE1 forms (Keil et al. 1985) (Fig. 2a, b). Further markers used were early-phase (m04/gp34) (Berry et al. 2014) (Fig. 2b) and the mid- to late-phase viral tegument protein (m25) (Kutle et al. 2017) (Fig. 3b). In parallel, we used the mouse embryonic fibroblasts (MEFs) to follow the distinct parameters of MCMV infection representing our previously established virus-cell interaction as a control model in our laboratory. Most infected cells displayed a distinctive round-shape morphology present in both cell phenotypes (Fig. 2a), corresponding to the well-known virus-induced cytopathogenic effect (Kutle et al. 2017). This was particularly noticeable in the "reversion" of the ramified morphology in the BV-$2^{\varnothing FCS}$ cells to an ameboid-like morphology (Fig. 2a *in box*). Measuring viral infection marker expressions over a 24-h time period revealed a slight delay in appearance and a higher degree of protein expression by Western blot in the BV-$2^{FCShigh}$ cells (Fig. 2b). However, the expression kinetics revealed a significant delay for the appearance of all viral protein compared to MEF cells (not shown).

Although the virus titer was displayed within a quite high range on the log scale, the productivity of infection for both BV-2 cell populations was lower than in MEF cultures (Fig. 2c). The microglia shares the features of immune cells in the CNS with the surface expression of MHC class I molecules as the main properties of antigen-presenting cells to contribute to T cell-mediated immunity (Malo et al. 2018). Therefore, we tested the MCMV immunosuppressive mechanism based on MHC-I downregulation as a molecular target for viral evasion of immune response (Wagner et al. 2002). In baseline conditions both BV-$2^{\varnothing FCS}$ and BV-$2^{FCShigh}$ have a high surface expression of MHC-I, which MCMV reduces from the cell surface (Fig. 3d), inducing the MHC-I immune-suppressed phenotype. On the other hand, MHC-II expression is non-existent in baseline conditions, and readily increases in response to the MCMV infection (Fig. 3d). Other analyzed cell surface molecules were not modulated in infected cells (Fig. 3d) due to a viral selective effect visible on the cell surface or an insufficient screening for viral cell surface molecular targets on the cell membrane.

MCMV induces immune-suppressive and metabolically activated phenotype in microglia

Our next goal was to determine whether the virus modulates the activation and metabolic state of the cells, along with the previously mentioned immunomodulation.

We analyzed the expression of protein markers, iNOS, Arg-1, CD206, and HIF-1α in MCMV-infected cells 24 h post-infection to elucidate the virus-induced changes associated with the cell activation (Fig. 3a). In BV-$2^{\varnothing FCS}$ cells the iNOS/Arg-1 expression was modulated leading to a reversal of the $iNOS^{low}Arg1^{high}$ phenotype compared to the uninfected cells (Fig. 3a). This molecular expression turnover indicates the viral potential to induce the changes in cellular proteomics to gain specific resources for its own biosynthesis needs. Arg-1 overall expression in infected cells was not significantly altered compared to uninfected cells; however, most infected cells had an appearance of distinct nuclear localization and an expression pattern that was not present in the non-infected cells (Fig. 3a). An Arg-1 nucleolar localization was specified in co-localization experiment performed by overlapping with the both nucleolar viral marker proteins, E-1, that we used as a an early nucleolar-expressed viral protein (Bühler et al. 1990) (not shown) and m25 nucleolar-expressed protein in the mid to late phase of infection (Kutle et al. 2017). Accumulation of highly expressed Arg-1 distributed in a punctuate form within the nucleolus occurred in the mid to late phase (12–16 h) of infection, with the coexpression of m25 viral protein (Fig. 3b). At the same time, we observed larger non-infected cells exhibiting even higher levels of iNOS expression surrounded by the infected cells (Fig. 3a). To support this belief, we added IFN-γ to the cell cultures and induced changes reflected with more ramified morphology and a significant increase of iNOS expression (supplementary data). Additionally, the cells pretreated with IFN-γ were less permissive to MCMV infection, indicating that paracrine IFN-γ signaling is required to induce a cell's defensive mode against infection (supplementary data). On the contrary, MCMV infection did not change the expression of CD206 (Fig. 3a, d), indicating that the virus does not alter the cell activation state in the "common sense" of microglial polarization. At the same time, BV-$2^{FCShigh}$ cells were quite uniformed in exhibiting the **$iNOS^{high}Arg1^{mid}CD206^{high}$** phenotypic characteristics. All infected cells exhibited high expressions of HIF-1α in both cultivation conditions, indicating a metabolic transition towards aerobic glycolysis within a metabolically activated phenotype (Fig. 3c) that usually occurs in microglia cells as well upon danger stimuli (Burns and Manda 2017). We confirmed that infected cells have an increased baseline glycolysis, but also less spare

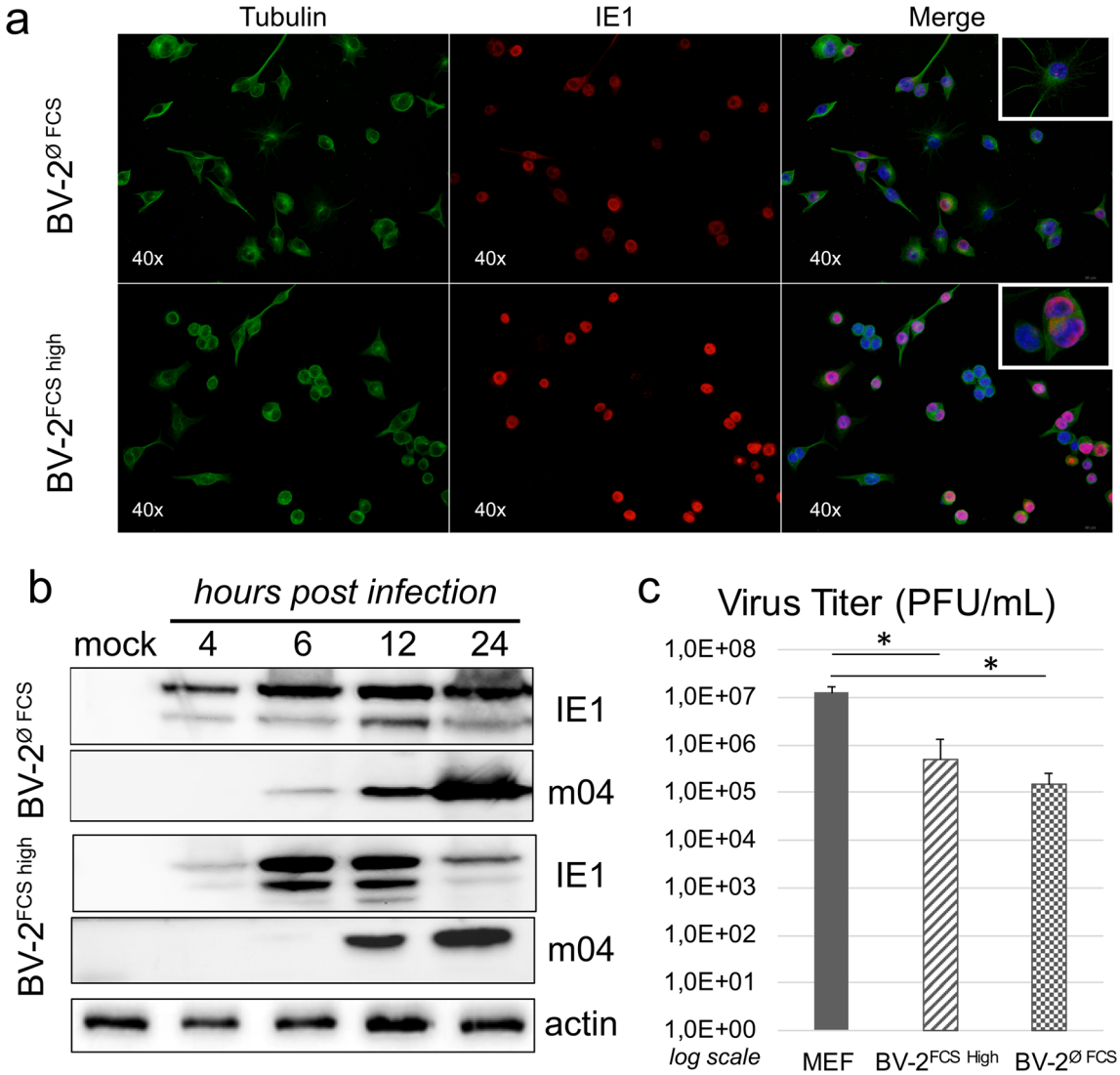

Fig. 2 BV-2 microglial cells susceptibility to murine cytomegaloviral infection. **a** Detection and nuclear localization of MCMV immediate-early 1 (IE1) protein in the microglial BV-2 cells as a marker of infection. BV-2 microglial cells were infected by MCMV at 10 m.o.i. and immunostained with a primary antibody directed against the MCMV-IE1 and a secondary Alexa Fluor 555 labeled antibody (*red signal*) at 24 h post-infection. Tubulin was used for cytoplasmic counterstaining (*green signal*) and DAPI for nuclear staining (*blue signal*). Immunofluorescent staining was performed for the control at the same time point. Original magnification was ×40. The representative cells are posted inside the window box frames displaying a distinct morphology of BV-2^{ØFCS} and BV-2^{FCShigh} cells. Notable characteristic cytopathogenic effects of MCMV infection can be seen in progressive morphology changes that occur in infected cells in later time frames, which obtain distinctive ameboid morphology. **b** Delayed expression kinetics of MCMV-IE1 and early protein (m04) in BV-2 cells. Western blot analysis of viral infection marker protein IE1 and early infection protein (m04) in infected BV-2^{Ø} ^{FCS} cells show that the expression of IE1 starts at 4 h followed by the expression of m04 at 8 h p.i. In parallel the expression of IE1 in infected BV-2^{FCShigh} starts at 6 h followed by the expression of m04 at 12 h p.i. Actin was used as a loading control. **c** Productive infection in BV-2 cells. Third-passage mouse embryonic fibroblasts (MEFs), prepared from BALB/c mice as well as BV-2^{ØFCS} and BV-2^{FCShigh}, were infected with the Smith strain wild-type MCMV at 10 m.o.i. Supernatants were harvested 24 h. p.i., and virus titers were determined by a standard plaque forming unit (p.f.u.) assay. Mean values of three independent experiments and SEM values of four replicates are shown. All cells supported the replication of MCMV with extracellular production of virus by 24 h p.i. and virus titer (up to 10^5–10^8) reached a maximum day 3 post-infection

glycolytic potential due to their metabolic activation (Fig. 3c) by using a real-time metabolic assay.

Finally, this data indicates that MCMV infection significantly alters the immunometabolic phenotypic properties of BV-2 microglia cells.

Discussion

In basal homeostatic in vivo conditions microglia cell morphology is predominantly ramified, with slight differences regarding their location in the brain (Fernández-Arjona et al. 2017). We

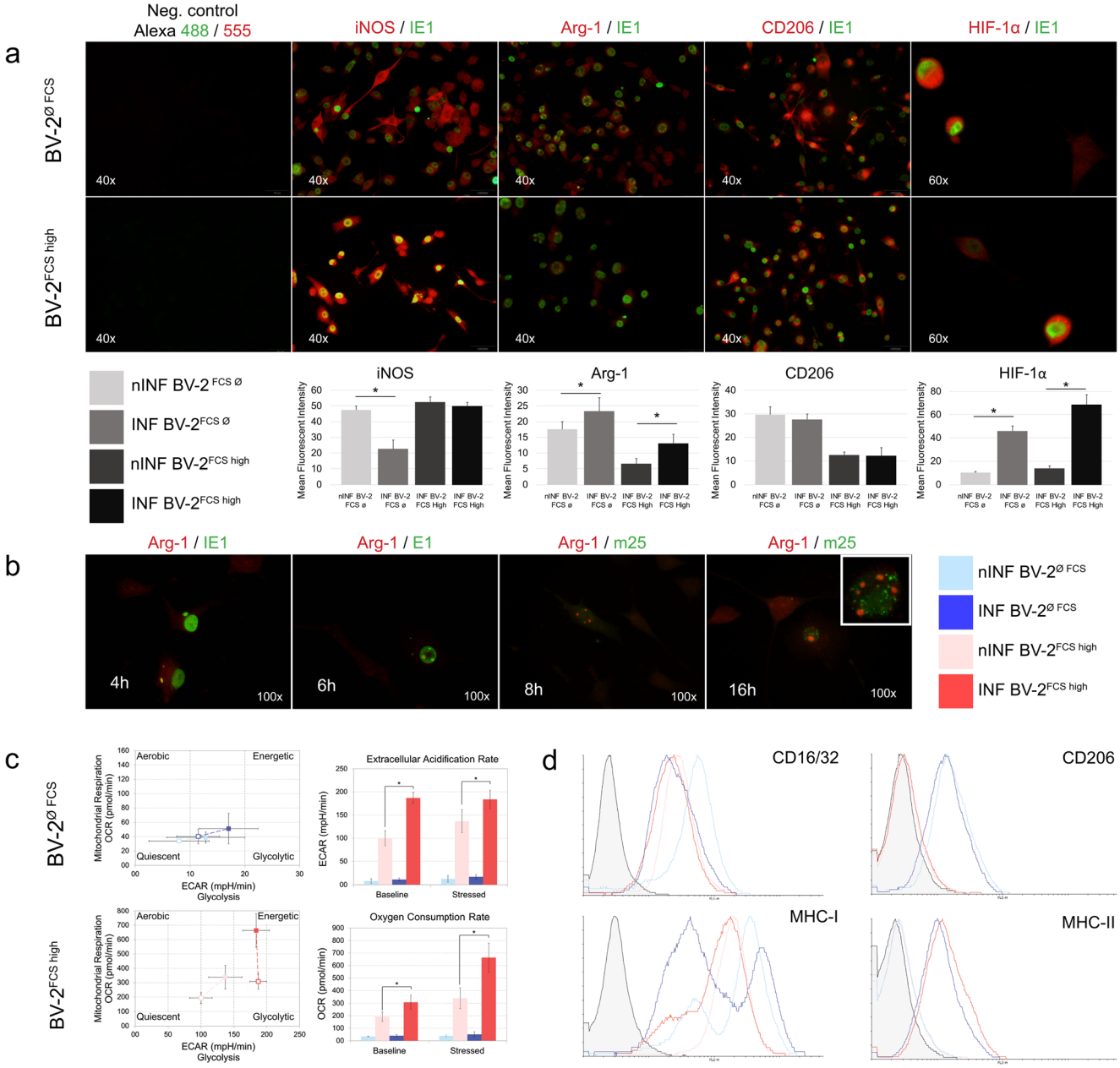

Fig. 3 Immunometabolic changes induced in BV-2 microglial cells upon murine cytomegaloviral infection. **a** Immunofluorescence of infected BV-2 microglial cells cultivated in two different conditions, in DMEM media supplemented with 10% FCS (BV-$2^{FCShigh}$) or without FCS (BV-$2^{\varnothing FCS}$). Viral infection causes an increase of iNOS in non-infected cells surrounding the infected ones, while the infected cells themselves do not exhibit an increase in iNOS expression in BV-$2^{\varnothing FCS}$ cells. Furthermore, Arg-1 and HIF-1α expression was significantly increased in both cultivated conditions upon cytomegaloviral infection, while the expression of CD206 was unchanged. Therefore, the infected BV-$2^{\varnothing FCS}$ exhibited an $iNOS^{low}$, Arg-1^{high}, $CD206^{high}$, and HIF-$1\alpha^{high}$ phenotype, while the infected BV-$2^{FCShigh}$ exhibited an $iNOS^{high}$, Arg-1^{mid}, $CD206^{low}$, and HIF-$1\alpha^{high}$ phenotype. **b** Nucleolar expression of Arg-1 is present in infected BV-2 microglia cells, confirmed by the colocalization with the nucleolar viral infection markers (E1 and m25). Characteristic Arg-1 nucleolar-associated expression in a dotted-shape form appears in cells from the 12–16 h marked (*shown in box*) and present in all cells expressing positive m25 viral protein till the end of viral replication cycle. **c** Cell energy phenotype of infected and non-infected cells, based on the real-time metabolism assay, reveals a statistically significant increase in aerobic and anaerobic metabolism in infected BV-$2^{FCShigh}$ cells. The same occurred in BV-$2^{\varnothing FCS}$, albeit at smaller scale, as the cells remained mostly quiescent. **d** Flow cytometry analysis of cell surface markers confirmed the expression of CD206 previously shown with immunofluorescence. CD16/32 was slightly downregulated in infected BV-$2^{\varnothing FCS}$ and BV-$2^{FCShigh}$ compared to control. A similar downregulation can be seen in the MHC-I surface expression, while MHC-II was upregulated upon cytomegaloviral infection in both cultivation conditions

found that adjusting the cultivation conditions by cultivating cells in serum-free medium causes a gradual shift in morphology towards a more ramified state. Recent studies confirm that serum exposure greatly alters microglia morphology and function, similar to our observation (Bohlen et al. 2017). As mentioned earlier, we hypothesize that this could be due to one of the prime constituents of FCS, Fetuin A, which is a known TLR-4 activator (Pal et al. 2012). However, it is difficult to test which constituent could be responsible for this effect due to the differences between each batch of FCS (Gstraunthaler et al. 2013). With the purpose to characterize these cells we have tried to achieve an appropriate condition as close as possible to those found in basal homeostatic state in vivo. Thus, microglia was characterized by morphological features that in a quite good extent reflect their functional capacity. Along with the observation that activation state affected microglia morphology we also found distinct changes in the phenotype with BV-$2^{FCS\ high}$ cells displaying a **iNOS^{high}Arg-1^{low}CD206^{low}HIF-1α^{high}**, while the BV-$2^{\varnothing FCS}$ exhibited a **iNOS^{low}Arg-1^{high}CD206^{high}HIF-1α^{low}**. By using this approach, cells were uniformed within differently associated phenotype. Expressions of markers in BV-$2^{FCS\ high}$ are consistent with numerous studies that point out the importance of iNOS in microglial activation wherein iNOS does indicate a pro-inflammatory phenotype, while the opposite is true for quiescent ramified cells (Pawate et al. 2004; Sierra et al. 2014). Metabolic activity to sustain such a state is fuelled by increased glycolytic metabolism via HIF-1α, as a strong enhancer of glycolysis (Wang et al. 2017), whose expression was increased in the BV-$2^{FCS\ high}$ compared to the BV-$2^{\varnothing FCS}$ cells in our study. On the other hand, removing the serum from the media increased the expression of Arg-1 and CD206, markers commonly used to indicate a repair and regeneration phenotype (Chhor et al. 2013; Cherry et al. 2014). Lastly, we wanted to confirm the distinct phenotypes with a metabolic analysis, since cell metabolism states greatly dictate the possible function of macrophages and microglia alike (Zhu et al. 2015). The BV-$2^{FCS\ high}$ cells exhibited a metabolically active, glycolytic state, consistent with a pro-inflammatory phenotype described by Orihuela et al. (2016). Curiously, the BV-$2^{\varnothing FCS}$ displayed a complete quiescent profile with general metabolic inactivity, which is not consistent with the high oxidative metabolism of the regenerative phenotype that we initially anticipated (Orihuela et al. 2016; Galván-Peña and O'Neill 2014).

In our study, cells retained the metabolic potential upon stimulation in both cultivating conditions, so we expected them to be fit for further experiments with MCMV infection.

Despite common beliefs that the steady-state microglia is static, recent studies have characterized the quiescent phenotype as quite a dynamic state (Lively and Schlichter 2013) characterized by an increased expression of oxidative genes that could favor cellular defense against viral attacks. This could explain the weaker expression of the IE1 and m04 viral proteins during the viral replication cycle followed by a slightly lower productivity of infection in quiescent BV-$2^{\varnothing FCS}$ cells (Fig. 2b, c). Otherwise, the glycolitically active BV-$2^{FCShigh}$ cells exhibit a delayed IE1 expression indicating a lower cell susceptibility to MCMV. This was followed by higher IE1 and m04 protein expression and ultimately higher productivity of infection (Fig. 2b, c). Thus, similar to cellular requirements for metabolic changes in shifting from a quiescent to a proliferating state, the virus also demands metabolic adaptations regarding energy utilization and mitochondrial energetic modulation (Sanchez and Lagunoff 2015). Other metabolomic studies have described a close relationship between viral components of different viruses with the mitochondrion as a metabolic factory of the cell (El-Bacha and Da Poian 2013). Differences in cell susceptibility to viral infection between BV-$2^{FCS\ high}$ and BV-$2^{\varnothing FCS}$ could be associated with their distinct M1- and M2-like phenotype based on the metabolic program altered by virus-cell interaction. Divergent cell permissiveness has been reported in HCMV infection model of human macrophages with optimal susceptibility in M2 polarized macrophages (Poglitsch et al. 2012).

In comparison to the primary murine microglial cells that are confirmed to be fully permissive to MCMV replication with supportive productive infection (Schut et al. 1994), we found that the BV-2 microglia cell line is much less susceptible to MCMV infection. This is also evident in regard to the mouse embryonic fibroblasts as a comparative model for MCMV-cell biology, which is well characterized in our laboratory. In MCMV-infected fibroblasts we investigated downregulated MHC-I cell phenotype as a result of the viral immune evasive proteins that account for MHC class I degradation and intracellular retention (Kučić et. al), which correlates with the decreased MHC-I expression in MCMV-infected BV-2 microglia cells (Fig. 3d). Additionally, upregulated MHC-II phenotype was present in BV-2-infected cells. Furthermore, viral and metabolic cell reprogramming that underlies the affected cell immune status refers also to the cell activation state that is not strictly covered by M1/M2 microglial polarization profile.

Interestingly, non-infected BV-$2^{\varnothing FCS}$ cells surrounded by infected BV-$2^{\varnothing FCS}$ cells exhibited a much higher iNOS expression compared to control or infected cells. We hypothesized that this could be the cause of this increased expression as a paracrine defense mechanism knowing that microglia can secrete IFNγ as a defense mechanism against other viral infections (Tsai et al. 2016). IFNγ-stimulated cells exhibited a high expression of iNOS and M1-like properties to induce a cell's defensive mode against infection (supplementary data), similar to those found in the literature (Schut et al. 1994). Furthermore, IFNγ preconditioning increases the resistance of BV-2 microglial cells to MCMV infection in both cultivation conditions (supplementary data), which is an already known effect of IFNγ prestimulation (Schut et al. 1994) and a defense mechanism that could be a possible reason for high iNOS expression. It is also known that IFNγ inhibits murine cytomegalovirus infection by blocking the

viral immediate-early promoter activity (Kropp et al. 2011), as a part of a defensive reaction against the virus in primary macrophages. Therefore, the increased iNOS expression in the non-infected BV-$2^{\varnothing FCS}$ appears to be induced by the nearby cells as protection against spreading of the viral infection. It is important to note that this inhibition, which occurs through synergistic IFN signaling, is known to be completely reversible and could have implications in establishing CMV latency (Dağ et al. 2014).

Furthermore, an increased accumulation of Arg-1 was observed in the nucleolus of infected cells, starting from 6 h post-infection. To our best knowledge, there is no research covering this specific localization of Arg-1, other than Monty et al. who mentions that a portion of this enzyme in the liver has nucleolar localization (Monty et al. 1956). Arg-1 is known for its role in metabolizing arginine to ornithine (Chang et al. 1998), a function that causes a depletion of substrate for nitric oxide synthases (NOS) and a decrease in nitric oxide (NO), which plays an important role in wound healing and immune response (Witte and Barbul 2003). Arginine metabolism in general plays a crucial role in shaping both innate and adaptive immunity, and an increase in Arg-1 expression does shift the cell towards a more anti-inflammatory state with increased synthesis of polyamines and proline (Rodriguez et al. 2017). Interestingly, recent studies have shown that two isoforms of arginase are involved in regulation of arginine metabolism (Morris 2009). Arg-1 plays an important role in viral infections, as a genetic ablation of Arg-1 in macrophages enhances viral clearance (Stoermer et al. 2012). Furthermore, Arg-1 upregulation can be seen in hepatitis C virus as well, which contributes to the viral carcinogenesis in the liver (Cao et al. 2009). For HCMV infection has been shown to upregulate arginase-2 (Arg-2) in endothelial, which is a mitochondrial enzyme with similar functions to Arg-1 (Yaiw et al. 2014). Arg-1 nucleolar expression in our study was seen in all cells with a positive viral m25 protein expression (Fig. 3b), indicating that the accumulation precedes a shift to middle-late infection phase and could be an important step for viral replication, bearing in mind that viruses must activate the appropriate biosynthetic pathways for synthesis of a new virion. Taken together, it seems that Arg-1 has a function in both the metabolic regulation of cell activity and polarization towards M2-like phenotype, along with a role in MCMV infection that needs to be thoroughly explored and assessed with the aim to determine whether modulation in arginine metabolism benefits the host or the virus. Conclusively, metabolism directly regulates immune functions in infected immune cells towards appropriate immune-metabolic phenotypes.

Conclusions

- Morphological features of BV-2 microglia cells reflect their functional capacity (cells cultivated without FCS, BV-$2^{\varnothing FCS}$ go through a morphologic and functional shift towards an quiescent M2-like ramified state).
- Distinct cell phenotype was associated with the activated BV-$2^{FCS\ high}$ cells displaying a iNOS^{high}Arg-1^{low}CD206^{low}HIF-1α^{high}, while the quiescent BV-$2^{\varnothing FCS}$ cells exhibited a iNOS^{low}Arg-^{high}CD206^{high}HIF-1α^{low} phenotype.
- BV-$2^{FCS\ high}$ cells exhibited a metabolically active, glycolytic state, consistent with a M1-like pro-inflammatory phenotype were less permissive to MCMV infection than metabolically inactive, quiescent BV-$2^{\varnothing FCS}$ cells, consistent with a M2-like as an MCMV-permissive phenotype.
- Although the expression strength does not change significantly in infected cells, they exhibit a special Arg-1 nucleolar pattern in both cell phenotypes.

Funding information This work was supported by the University of Rijeka Grant No. 13.06.1.3.45.

Compliance with ethical standards

Conflict of interest The authors declare that they have no conflicts of interest.

References

Artyomov MN, Sergushichev A, Schilling JD (2016) Integrating immunometabolism and macrophage diversity. Semin Immunol 28:417–424. https://doi.org/10.1016/j.smim.2016.10.004

Berry R, Vivian JP, Deuss FA, Balaji GR, Saunders PM, Lin J, Littler DR, Brooks AG, Rossjohn J (2014) The structure of the cytomegalovirus-encoded m04 glycoprotein, a prototypical member of the m02 family of immunoevasins. J Biol Chem 289:23753–23763. https://doi.org/10.1074/jbc.M114.584128

Blasi E, Barluzzi R, Bocchini V, Mazzolla R, Bistoni F (1990) Immortalization of murine microglial cells by a *v-raf/v-myc* carrying retrovirus. J Neuroimmunol 27(1990):229–237. https://doi.org/10.1016/0165-5728(90)90073-V

Bohlen CJ, Bennett FC, Tucker AF, Collins HY, Mulinyawe SB, Barres BA (2017) Diverse requirements for microglial survival, specification, and function revealed by defined-medium cultures. Neuron 94:759–773.e8. https://doi.org/10.1016/J.NEURON.2017.04.043

Bühler B, Keil GM, Weiland F, Koszinowski UH (1990) Characterization of the murine cytomegalovirus early transcription unit e1 that is induced by immediate-early proteins. J Virol 64:1907–1919

Burns JS, Manda G (2017) Metabolic pathways of the Warburg effect in health and disease: perspectives of choice, chain or chance. Int J Mol Sci 18:2755. https://doi.org/10.3390/ijms18122755

Busche A, Angulo A, Kay-Jackson P, Ghazal P, Messerle M (2008) Phenotypes of major immediate-early gene mutants of mouse cytomegalovirus. Med Microbiol Immunol 197:233–240. https://doi.org/10.1007/s00430-008-0076-3

Cadena-Herrera D, Esparza-De Lara JE, Ramírez-Ibañez ND, López-Morales CA, Pérez NO, Flores-Ortiz LF, Medina-Rivero E (2015) Validation of three viable-cell counting methods: manual, semi-automated, and automated. Biotechnol Rep 7:9–16. https://doi.org/10.1016/j.btre.2015.04.004

Cao W, Sun B, Feitelson MA, Wu T, Tur-Kaspa R, Fan Q (2009) Hepatitis C virus targets over-expression of arginase I in hepatocarcinogenesis. Int J Cancer 124:2886–2892. https://doi.org/10.1002/ijc.24265

Chang CI, Liao JC, Kuo L (1998) Arginase modulates nitric oxide production in activated macrophages. Am J Phys 274:H342–H348

Cheeran MC, Hu S, Yager SL, Gekker G, Peterson PK, Lokensgard JR (2001) Cytomegalovirus induces cytokine and chemokine production differentially in microglia and astrocytes: antiviral implications. J Neuro-Oncol 7:135–147. https://doi.org/10.1080/13550280152058799

Cherry JD, Olschowka JA, O'Banion MK (2014) Neuroinflammation and M2 microglia: the good, the bad, and the inflamed. J Neuroinflammation 11:98. https://doi.org/10.1186/1742-2094-11-98

Chhor V, Le Charpentier T, Lebon S, Oré M-V, Celador IL, Josserand J, Degos V, Jacotot E, Hagberg H, Sävman K, Mallard C, Gressens P, Fleiss B (2013) Characterization of phenotype markers and neuronotoxic potential of polarised primary microglia in vitro. Brain Behav Immun 32:70–85. https://doi.org/10.1016/j.bbi.2013.02.005

Cloarec R, Bauer S, Luche H, Buhler E, Pallesi-Pocachard E, Salmi M, Courtens S, Massacrier A, Grenot P, Teissier N, Watrin F, Schaller F, Adle-Biassette H, Gressens P, Malissen M, Stamminger T, Streblow DN, Bruneau N, Szepetowski P (2016) Cytomegalovirus infection of the rat developing brain in utero prominently targets immune cells and promotes early microglial activation. PLoS One 11:e0160176. https://doi.org/10.1371/journal.pone.0160176

Cloarec R, Bauer S, Teissier N, Schaller F, Luche H, Courtens S, Salmi M, Pauly V, Bois E, Pallesi-Pocachard E, Buhler E, Michel FJ, Gressens P, Malissen M, Stamminger T, Streblow DN, Bruneau N, Szepetowski P (2018) In utero administration of drugs targeting microglia improves the neurodevelopmental outcome following cytomegalovirus infection of the rat fetal brain. Front Cell Neurosci 12:55. https://doi.org/10.3389/fncel.2018.00055

Dağ F, Dölken L, Holzki J, Drabig A, Weingärtner A, Schwerk J, Lienenklaus S, Conte I, Geffers R, Davenport C, Rand U, Köster M, Weiß S, Adler B, Wirth D, Messerle M, Hauser H, Cičin-Šain L (2014) Reversible silencing of cytomegalovirus genomes by type I interferon governs virus latency. PLoS Pathog 10:e1003962. https://doi.org/10.1371/journal.ppat.1003962

Das Sarma J (2014) Microglia-mediated neuroinflammation is an amplifier of virus-induced neuropathology. J Neuro-Oncol 20:122–136. https://doi.org/10.1007/s13365-013-0188-4

Doke SK, Dhawale SC (2015) Alternatives to animal testing: a review. Saudi Pharm J 23:223–229. https://doi.org/10.1016/J.JSPS.2013.11.002

El-Bacha T, Da Poian AT (2013) Virus-induced changes in mitochondrial bioenergetics as potential targets for therapy. Int J Biochem Cell Biol 45:41–46. https://doi.org/10.1016/j.biocel.2012.09.021

Fernández-Arjona MDM, Grondona JM, Granados-Durán P, Fernández-Llebrez P, López-Ávalos MD (2017) Microglia morphological categorization in a rat model of neuroinflammation by hierarchical cluster and principal components analysis. Front Cell Neurosci 11:235. https://doi.org/10.3389/fncel.2017.00235

Fleck-Derderian S, McClellan W, Wojcicki JM (2017) The association between cytomegalovirus infection, obesity, and metabolic syndrome in U.S. adult females. Obesity 25:626–633. https://doi.org/10.1002/oby.21764

Galván-Peña S, O'Neill LAJ (2014) Metabolic reprograming in macrophage polarization. Front Immunol 5:420. https://doi.org/10.3389/fimmu.00420

Ginhoux F, Greter M, Leboeuf M, Nandi S, See P, Gokhan S, Mehler MF, Conway SJ, Ng LG, Stanley ER, Samokhvalov IM, Merad M (2010) Fate mapping analysis reveals that adult microglia derive from primitive macrophages. Science 330:841–845. https://doi.org/10.1126/science.1194637

Gstraunthaler G, Lindl T, van der Valk J (2013) A plea to reduce or replace fetal bovine serum in cell culture media. Cytotechnology 65:791–793. https://doi.org/10.1007/s10616-013-9633-8

Guruswamy R, ElAli A (2017) Complex roles of microglial cells in ischemic stroke pathobiology: new insights and future directions. Int J Mol Sci 18:496. https://doi.org/10.3390/ijms18030496

Hanisch U-K, Kettenmann H (2007) Microglia: active sensor and versatile effector cells in the normal and pathologic brain. Nat Neurosci 10:1387–1394. https://doi.org/10.1038/nn1997

Henn A, Lund S, Hedtjärn M, Schrattenholzer A, Pörzgen P, Leist M (2009) The suitability of BV2 cells as alternative model system for primary microglia cultures or for animal experiments examining brain inflammation. ALTEX 26:83–94. https://doi.org/10.14573/altex.2009.2.83

Jonjic S (2015) CMV immunology. Cell Mol Immunol 12:125–127. https://doi.org/10.1038/cmi.2014.132

Jordan S, Krause J, Prager A, Mitrovic M, Jonjic S, Koszinowski UH, Adler B (2011) Virus progeny of murine cytomegalovirus bacterial artificial chromosome pSM3fr show reduced growth in salivary glands due to a fixed mutation of MCK-2. J Virol 85:10346–10353. https://doi.org/10.1128/JVI.00545-11

Keil GM, Fibi MR, Koszinowski UH (1985) Characterization of the major immediate-early polypeptides encoded by murine cytomegalovirus. J Virol 54:422–428

Kettenmann H, Hanisch U-K, Noda M, Verkhratsky A (2011) Physiology of microglia. Physiol Rev 91:461–553. https://doi.org/10.1152/physrev.00011.2010

Kropp KA, Robertson KA, Sing G, Rodriguez-Martin S, Blanc M, Lacaze P, Hassim MF, Khondoker MR, Busche A, Dickinson P, Forster T, Strobl B, Mueller M, Jonjic S, Angulo A, Ghazal P (2011) Reversible inhibition of murine cytomegalovirus replication by gamma interferon (IFN-γ) in primary macrophages involves a primed type I IFN-signaling subnetwork for full establishment of an immediate-early antiviral state. J Virol 85:10286–10299. https://doi.org/10.1128/JVI.00373-11

Kutle I, Sengstake S, Templin C, Glass M, Kubsch T, Keyser K, Binz A, Bauerfeind R, Sodeik B, Cicin-Sain L, Dezeljin M, Messerle M (2017) The M25 gene products are critical for the cytopathic effect of mouse cytomegalovirus. Sci Rep 7:15588. https://doi.org/10.1038/s41598-017-15783-x

Lively S, Schlichter LC (2013) The microglial activation state regulates migration and roles of matrix-dissolving enzymes for invasion. J Neuroinflammation 10:843. https://doi.org/10.1186/1742-2094-10-75

Loftus RM, Finlay DK (2016) Immunometabolism: cellular metabolism turns immune regulator. J Biol Chem 291:1–10. https://doi.org/10.1074/jbc.R115.693903

Lucin P, Jonjić S (1995) Cytomegalovirus replication cycle: an overview. Period Biol 97:13–22

Malo CS, Jin F, Hansen MJ, Fryer JD, Pavelko KD, Johnson AJ (2018) MHC class I expression by microglia is required for generating a complete antigen-specific CD8 T cell response in the CNS. J Immunol 200:99.7

Marín-Teva JL, Dusart I, Colin C, Gervais A, van Rooijen N, Mallat M (2004) Microglia promote the death of developing Purkinje cells. Neuron 41:535–547. https://doi.org/10.1016/S0896-6273(04)00069-8

Mathis D, Shoelson SE (2011) Immunometabolism: an emerging frontier. Nat Rev Immunol 11:81–83. https://doi.org/10.1038/nri2922

Miyamoto A, Wake H, Ishikawa AW, Eto K, Shibata K, Murakoshi H, Koizumi S, Moorhouse AJ, Yoshimura Y, Nabekura J (2016) Microglia contact induces synapse formation in developing somatosensory cortex. Nat Commun 7:12540. https://doi.org/10.1038/ncomms12540

Monty KJ, Litt M, Kay ER, Dounce AL (1956) Isolation and properties of liver cell nucleoli. J Biophys Biochem Cytol 2:127–145. https://doi.org/10.1083/jcb.2.2.127

Morris SM Jr (2009) Recent advances in arginine metabolism: roles and regulation of the arginases. Br J Pharmacol 157:922–930. https://doi.org/10.1111/j.1476-5381.2009.00278.x

Naing ZW, Scott GM, Shand A, Hamilton ST, van Zuylen WJ, Basha J, Hall B, Craig ME, Rawlinson WD (2016) Congenital cytomegalovirus infection in pregnancy: a review of prevalence, clinical features, diagnosis and prevention. Aust N Z J Obstet Gynaecol 56:9–18. https://doi.org/10.1111/ajo.12408

Orihuela R, McPherson CA, Harry GJ (2016) Microglial M1/M2 polarization and metabolic states. Br J Pharmacol 173:649–665. https://doi.org/10.1111/bph.13139

Pal D, Dasgupta S, Kundu R, Maitra S, Das G, Mukhopadhyay S, Ray S, Majumdar SS, Bhattacharya S (2012) Fetuin-A acts as an endogenous ligand of TLR4 to promote lipid-induced insulin resistance. Nat Med 18:1279–1285. https://doi.org/10.1038/nm.2851

Pawate S, Shen Q, Fan F, Bhat NR (2004) Redox regulation of glial inflammatory response to lipopolysaccharide and interferon? J Neurosci Res 77:540–551. https://doi.org/10.1002/jnr.20180

Poglitsch M, Weichhart T, Hecking M, Werzowa J, Katholnig K, Antlanger M, Krmpotic A, Jonjic S, Hörl WH, Zlabinger GJ, Puchhammer E, Säemann MD (2012) CMV late phase-induced mTOR activation is essential for efficient virus replication in polarized human macrophages. Am J Transplant 12:1458–1468. https://doi.org/10.1111/j.1600-6143.2012.04002.x

Ransohoff RM (2016) A polarizing question: do M1 and M2 microglia exist? Nat Neurosci 19:987–991. https://doi.org/10.1038/nn.4338

Reddehase MJ, Lemmermann NAW (2018) Mouse model of cytomegalovirus disease and immunotherapy in the immunocompromised host: predictions for medical translation that survived the "test of time". Viruses 10:693. https://doi.org/10.3390/v10120693

Reddehase MJ, Balthesen M, Rapp M, Jonjić S, Pavić I, Koszinowski UH (1994) The conditions of primary infection define the load of latent viral genome in organs and the risk of recurrent cytomegalovirus disease. J Exp Med 179:185–193. https://doi.org/10.1084/jem.179.1.185

Rock RB, Gekker G, Hu S, Sheng WS, Cheeran M, Lokensgard JR, Peterson PK (2004) Role of microglia in central nervous system infections. Clin Microbiol Rev 17:942–964. https://doi.org/10.1128/CMR.17.4.942-964.2004

Rodriguez PC, Ochoa AC, Al-Khami AA (2017) Arginine metabolism in myeloid cells shapes innate and adaptive immunity. Front Immunol 8:93. https://doi.org/10.3389/fimmu.2017.00093

Sanchez EL, Lagunoff M (2015) Viral activation of cellular metabolism. Virology 479–480:609–618. https://doi.org/10.1016/j.virol.2015.02.038

Schafer DP, Stevens B (2013) Phagocytic glial cells: sculpting synaptic circuits in the developing nervous system. Curr Opin Neurobiol 23:1034–1040. https://doi.org/10.1016/J.CONB.2013.09.012

Schut RL, Gekker G, Hu S, Chao CC, Pomeroy C, Jordan MC, Peterson PK (1994) Cytomegalovirus replication in murine microglial cell cultures: suppression of permissive infection by interferon-gamma. J Infect Dis 169:1092–1096

Sierra A, Navascués J, Cuadros MA, Calvente R, Martín-Oliva D, Ferrer-Martín RM, Martín-Estebané M, Carrasco M-C, Marín-Teva JL (2014) Expression of inducible nitric oxide synthase (iNOS) in microglia of the developing quail retina. PLoS One 9:e106048. https://doi.org/10.1371/journal.pone.0106048

Slavuljica I, Kveštak D, Csaba Huszthy P, Kosmac K, Britt WJ, Jonjic S (2015) Immunobiology of congenital cytomegalovirus infection of the central nervous system—the murine cytomegalovirus model. Cell Mol Immunol 12:180–191. https://doi.org/10.1038/cmi.2014.51

Stansley B, Post J, Hensley K (2012) A comparative review of cell culture systems for the study of microglial biology in Alzheimer's disease. J Neuroinflammation 9:577. https://doi.org/10.1186/1742-2094-9-115

Stoermer KA, Burrack A, Oko L, Montgomery SA, Borst LB, Gill RG, Morrison TE (2012) Genetic ablation of arginase 1 in macrophages and neutrophils enhances clearance of an arthritogenic alphavirus. J Immunol 189:4047–4059. https://doi.org/10.4049/jimmunol.1201240

Teissier N, Fallet-Bianco C, Delezoide A-L, Laquerrière A, Marcorelles P, Khung-Savatovsky S, Nardelli J, Cipriani S, Csaba Z, Picone O, Golden JA, Van Den Abbeele T, Gressens P, Adle-Biassette H (2014) Cytomegalovirus-induced brain malformations in fetuses. J Neuropathol Exp Neurol 73:143–158. https://doi.org/10.1097/NEN.0000000000000038

Timmerman R, Burm SM, Bajramovic JJ (2018) An overview of in vitro methods to study microglia. Front Cell Neurosci 12:242. https://doi.org/10.3389/fncel.2018.00242

Tsai T-T, Chen C-L, Lin Y-S, Chang C-P, Tsai C-C, Cheng YL, Huang CC, Ho CJ, Lee YC, Lin LT, Jhan MK, Lin CF (2016) Microglia retard dengue virus-induced acute viral encephalitis. Sci Rep 6:27670. https://doi.org/10.1038/srep27670

Van den Pol AN, Reuter JD, Santarelli JG (2002) Enhanced cytomegalovirus infection of developing brain independent of the adaptive immune system. J Virol 76:8842–8854. https://doi.org/10.1128/JVI.76.17.8842-8854.2002

Wagner M, Gutermann A, Podlech J, Reddehase MJ, Koszinowski UH (2002) Major histocompatibility complex class I allele-specific cooperative and competitive interactions between immune evasion proteins of cytomegalovirus. J Exp Med 196:805–816. https://doi.org/10.1084/jem.20020811

Wagner FM, Brizic I, Prager A, Trsan T, Arapovic M, Lemmermann NA, Podlech J, Reddehase MJ, Lemnitzer F, Bosse JB, Gimpfl M, Marcinowski L, MacDonald M, Adler H, Koszinowski UH, Adler B (2013) The viral chemokine MCK-2 of murine cytomegalovirus promotes infection as part of a gH/gL/MCK-2 complex. PLoS Pathog 9:e1003493. https://doi.org/10.1371/journal.ppat.1003493

Wang T, Liu H, Lian G, Zhang S-Y, Wang X, Jiang C (2017) HIF1α-induced glycolysis metabolism is essential to the activation of inflammatory macrophages. Mediat Inflamm 2017:9029327. https://doi.org/10.1155/2017/9029327

Witte MB, Barbul A (2003) Arginine physiology and its implication for wound healing. Wound Repair Regen 11:419–423. https://doi.org/10.1046/j.1524-475X.2003.11605.x

Witting A, Müller P, Herrmann A, Kettenmann H, Nolte C (2000) Phagocytic clearance of apoptotic neurons by microglia/brain macrophages in vitro: involvement of lectin-, integrin-, and phosphatidylserine-mediated recognition. J Neurochem 75:1060–1070. https://doi.org/10.1046/j.1471-4159.2000.0751060.x

Yaiw K-C, Mohammad A-A, Taher C, Wilhelmi V, Davoudi B, Stråat K, Assinger A, Ovchinnikova O, Shlyakhto E, Rahbar A, Koutonguk O, Religa P, Butler L, Khan Z, Streblow D, Pernow J, Söderberg-Nauclér C (2014) Human cytomegalovirus induces upregulation of arginase II: possible implications for vasculopathies. Basic Res Cardiol 109:401. https://doi.org/10.1007/s00395-014-0401-5

Zhu L, Zhao Q, Yang T, Ding W, Zhao Y (2015) Cellular metabolism and macrophage functional polarization. Int Rev Immunol 34:82–100. https://doi.org/10.3109/08830185.2014.969421